Graft Copolymer Compatibilizers for Blends of Isotactic Polypropylene and Ethene-Propene Copolymers. 2. Functional Polymers Approach

Sudhin Datta*

Exxon Chemical Company, P.O. Box 45, Linden, New Jersey 07036

David J. Lohse

Exxon Research & Engineering Company, Route 22 East, Annandale, New Jersey 08801

Received October 12, 1992; Revised Manuscript Received January 19, 1993

ABSTRACT: A graft polymer with isotactic polypropylene (iPP) arms pendant from an ethene-propene (EP) copolymer backbone has been made and shown to effectively compatibilize EP/iPP blends. The synthesis of this molecule is by the reaction of mutually reactive functional polymeric components: a succinic anhydride grafted polypropylene is reacted with an EP containing primary amine groups, either in solution or in the melt state. This grafting has been demonstrated by infrared spectroscopy, solvent fractionation, and thermal analysis. The addition of less than 10% of this graft polymer to an iPP/EP blend has a large effect on its morphology and properties. Not only does the size of dispersed EP phase domains shrink by a factor of 4 when the compatibilizer is added but also the growth of the phase domains on thermal annealing in the melt is significantly reduced. The presence of the graft polymer in the interphase of the blend is shown directly by electron microscopy. Improvements in mechanical properties of iPP/EP blends containing compatibilizers have been noted. The low-temperature impact strength is increased, and the temperature of the transition from ductile to brittle behavior is reduced by up to 20 °C. Thus, such graft polymers work well as interfacial agents or compatibilizers to improve and stabilize blend properties.

Introduction

The field of polymer blends is developing rapidly, in terms of both scientific understanding and commerical utility. Existing polymers can be used in blends and alloys to provide materials[1] with a combination of properties unattainable in any single polymer. A blend morphology with 0.1-5-μm-diameter dispersed particles is usually required to attain most of the benefits. Structures significantly outside these limits show either only an average of component polymer properties or, more frequently, severe degradation in important properties. Within this range of morphology, the physical properties (mechanical, transport, or optical) of these materials depend crucially on the degree of dispersion. Thus the synergistic benefits of blending derive from the formation and retention of the appropriate blend morphology. Control of morphology is therefore control of polymer blend properties.

The long-chain nature of polymers leads to two competing thermodynamic and kinetic factors which affect the formation and stability of these micron-sized structures. First, the entropy of mixing for macromolecules is very small, so that most pairs of polymers are immiscible or insoluble in each other. Second, their chain structure also makes the dynamics of these mixtures very slow, so that complete phase separation of a blend takes a very long time. The combination of these two factors means that most polymer blends made by mixing either bulk polymers or solutions of polymers have a morphology of phase domains separated on the scale of 0.1-50 μm.

One of the largest classes of polymer blends in use today are the mixtures of isotactic polypropylene (iPP) and an ethene-propene copolymer (EP). Useful materials are obtained from blends over nearly the whole range of composition.[1-4] Blends with a small percentage of EP rubber are a toughened version of iPP, while those with a majority of EP are thermoplastic elastomers. Intermediate in composition are blends with a wide variety of stiffness, toughness, and other desirable physical properties. Thus, these versatile blends are important because of the wide range of desirable properties. The physical properties of the iPP/EP blends not only are a function of the blend composition but also depend on the morphology of the blend. The morphology depends on the blending procedure, the thermal history, and the characteristics (composition and molecular weight) of the polymers. This is because these polymers are immiscible, at least below the crystallization temperature of iPP[5] and generally in the melt as well.[6-8] They retain a two-phase morphology, and the sizes, shapes, and continuity of the phase domains determine the properties of the blend.

A way to control the morphology is through the use of "compatibilizers" which are block or graft polymers which are capable of acting as interfacial agents in polymer blends.[9-11] Usually, but not always, the blocks of the compatibilizer are identical with the blend components. These molecules are expected to be found at the interface of dissimilar polymers[10,12] because part of the compatibilizer is miscible with one component and part with the other. There are two effects of the presence of the compatibilizer at the interface: the adhesion between the phases increases[12] and the interfacial tension, γ, between them decreases.[13] At some level of compatibilizer incorporation γ drops to zero, so there is some finite, equilibrium size of the domains. Even when γ is nonzero, the fact that it is lower means that a finer dispersion of the phases can be achieved during intensive mixing.[14-16] The presence of the compatibilizer at the surface of the particles of the blend may also reduce phase growth by a steric stabilization mechanism.[15,17] The smaller phase size plus the increased phase adhesion results in improved physical properties such as impact strength[10,18,19] and tensile strength.[20]

The difficulty in making such compatibilizers for iPP/EP blends lies in the different characteristics of the two polymers and the differences in the synthesis of these apparently similar polyolefins. Isotactic iPP is a semicrystalline thermoplastic because it is made with a heterogeneous $TiCl_3$ catalyst that produces stereoregular

0024-9297/93/2226-2064$04.00/0

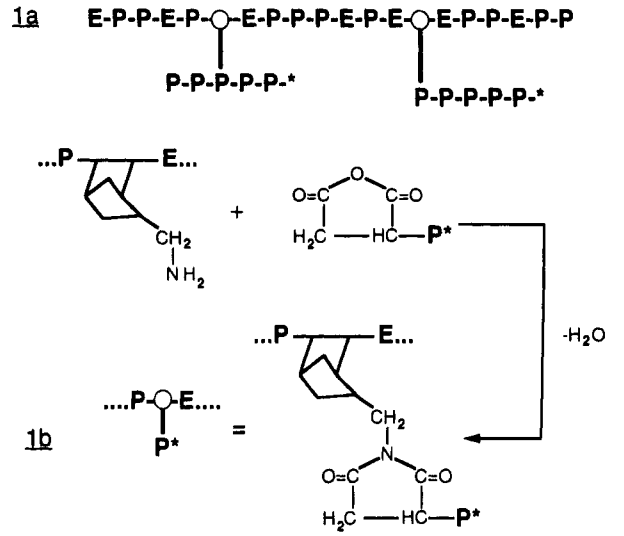

Figure 1. Structure (**1a**) and imidization reaction (**1b**) at the linking point for the EP-*g*-iPP polymer. P* is the polymeric fragment of the isotactic polypropene, and E and P are the ethene and propene residues of the ethene–propene copolymer.

incorporation of the methyl group of the propene monomer. The EP copolymers are commonly made with homogeneous vanadium-based catalysts that produce no stereoregularity; thus, the polymers are amorphous elastomers. Moreover, the Ziegler–Natta catalysts used to make these polyolefins do not exhibit polymerization kinetics (i.e., a "living" polymerization catalyst) that facilitate block polymer synthesis. Even the well-advertised "reactor block copolymer" polypropylenes are actually blends of iPP, EP, and sometimes polyethylene.[21] These contain an insignificant amount of a iPP–EP block polymer, if any. Thus, even though compatibilization of iPP/EP blends with a block polymer should give materials with improved properties, such polymeric surfactants are not synthetically accessible.

The synthetic target in this study was a graft copolymer of EP and iPP since it is possible to make the blocks separately and chemically couple them in a subsequent reaction. The graft polymer structures are shown as **1a** in Figure 1 where P* represents the polymeric iPP fragment. The graft polymers contain blocks of iPP pendant from the EP backbone.

In a previous paper we demonstrated a scheme to synthesize an EP–iPP graft polymer by a two-step process in which the EP part is made first and then the iPP is grown from it in the second step.[22] This was shown to be an effective means of producing such polymers, which functions as compatibilizers for EP/iPP blends. In this paper we demonstrate a second method to synthesize such graft polymers. In this procedure an EP containing a random primary amine functionality along the chain is reacted with the succinic anhydride functionality of a polypropylene which has been grafted in a free-radical condensation with maleic anhydride. These graft polymers are good compatibilizers for an iPP/EP blend. We demonstrate the ability of these compatibilizers to stabilize the size of dispersed EP domains and show directly that the graft polymers can be found at the interface in such blends. Further, the addition of these graft polymers leads to improvement in the mechanical properties of the iPP/EP blends; thus, the impact strength is improved and the ductile to brittle transition temperature for the iPP matrix is decreased by as much as 20 °C.

Experimental Section

Polymers. EP-amine. Primary amine functionalized EP polymer containing 51% ethene (EP-amine, Table I) was made by incorporation of the cyclic double bond of 5-(methylamino)-2-norbornene into the EP chain during the polymerization process. The primary amine groups are therefore pendant from the EP backbone. The synthesis and characterization of these polymers has been described elsewhere.[23] The formation of amine functionalized EPDM polymers containing 53% of ethene (EPDM-amine, Table I) is an extension of this synthetic procedure where the norbornene double bonds of both 5-(methylamino)-2-norbornene and 5-ethylidene-2-norbornene are incorporated into the EP backbone to yield both pendant primary amine and ethylidene functionalities. Both of these polymers are made with a soluble vanadium catalyst which has a single type of olefin polymerization site.[24] This produces a uniform composition (E/P ratio) for the entire polymer across the molecular weight distribution. These polymers are amorphous with only negligible amounts of crystallinity due to long methylene sequences. For both EP-amine and EPDM-amine polymers the distribution of amine groups is believed to be random along the polymer backbone. The concentration of amine groups is 0.3–0.5 mol % and measured in the infrared spectra by the absorbance due to N–H groups at 1619 cm^{-1}. The distribution of amine groups has been demonstrated (by UV–GPC)[23] to be uniform across the molecular weight distribution. For a polymer with a number-average molecular weight (M_n) of 40 000 this is equivalent to 3–5 amine groups/chain. The primary amine functionalized materials were used either as neat polymer for melt blending with other polymers or as a xylene solution containing 7–9% of polymer for solution reactions. Care was taken to exclude atmospheric CO_2, which rapidly reacts with amines, from the xylene solutions of the amine functional polymer prior to reaction with the anhydride functionality.

Table I
Molecular Weight Data[a] for Polymers

polymer	M_n	M_w	M_z	M_{z+1}
iPP-SA	16.7	64.0	152	323
EP-amine	30.7	54.5	62	89
EPDM-amine	39.1	82.3	100.7	122
EP-1	167.8	340.6	608.3	1037
PP-L	69.6	288.7	821.6	1637
PP-H	106.3	519.9	1394	2575

[a] Molecular weight data are $\times 10^3$.

Functional iPP. Succinic anhydride functionalized polypropylene (iPP-SA, Table I), made by grafting maleic anhydride to polypropylene in a free-radical process, was obtained from Himont Chemical Co. The kinetics of this condensation reaction[25] indicate that most of the anhydride groups are randomly located along the backbone of the iPP. However, there may be some preference for chain scission at the grafting site: this leads to terminal functionalization of iPP-SA. The interchain distribution of the anhydride concentration is not uniform, and there is an oligomeric fraction which is highly functionalized. iPP-SA with a more uniform distribution of functionality and suitable for our experiments is isolated from the commercial material by recrystallizing the polymer from hot xylene. The concentration of succinic anhydride groups was assayed from the IR spectra of a polymer film: the anhydride group has an intense absorbance[26] at 1840 cm^{-1} in the carbonyl region. Anhydrides are rapidly but reversibly hydrated to the diacid in the presence of atmospheric moisture, and the polymer films had to be heated to 150 °C for several minutes to complete the dehydration reaction for an accurate assay of the anhydride concentration. These polymers contain 1.10 mol % of succinic anhydride groups. For an iPP-SA molecule with a M_n of 15 000 this is equivalent to approximately 5 succinic anhydride groups/chain. The iPP-SA polymer was used either as neat polymer for melt blending with other polymers or as a xylene solution containing 7–9% of polymer for solution reactions.

Other Materials. Nonfunctional polymers such as EP-1, PP-L, and PP-H (Table I) were obtained from Exxon Chemical Co., Houston, TX. Irganox 1076 (I-1076), a hindered phenolic antioxidant, is available from Ciba-Geigy Co., Basel, Switzerland. 1-Dodecylamine was purchased from Aldrich Chemical Co.

Synthesis. Graft Polymer. Solution Synthesis. In a typical procedure for the synthesis of a 50:50 wt % composition graft of EP-amine and iPP-SA (Graft B, Table II) 68 g of iPP-SA was

Table II
Composition and Molecular Weight[a] of EP-g-iPP Graft Polymers and Nonreactive Blends

sample	composition	M_n	M_w	M_z	M_{z+1}
graft A	70 EP-amine/30 iPP-SA	22.2	129	686	2080
graft B	50 EP-amine/50 iPP-SA	18.9	133	358	671
graft C	35 EP-amine/65 iPP-SA	20.0	107	252	476
graft C*	30 EPDM-amine/70 iPP-SA				
blend D	30 EP-amine/70 PP-L				

[a] Molecular weight data are $\times 10^3$.

dissolved in 1.2 L of refluxing xylene containing 300 ppm of I-1076, in an atmosphere of nitrogen. Water was removed from the reflux condensate for 90 min through a Dean-Stark trap. To this solution was added 68 g of EP-amine as a 7% solution in xylene (approximately 1000 mL of solution), and the reflux continued for several (6–10) hours more. The progress of the reaction could be monitored by the presence of a trace of moisture in the reflux condensate; this was carefully removed. Very little moisture was visible after the first 3 h of reflux. At the end of the reflux very little, if any, of the polymer had formed a gel. The polymer solution was cooled to room temperature to form a clear gelatinous solution; there was no observable precipitation of the normally insoluble polypropylene even after several hours at room temperature. The polymer was recovered by evaporation of the solvent under vacuum at 60–70 °C.

Graft Polymer. Melt Synthesis. For the synthesis of a 50:50 wt % composition graft of EP-amine and iPP-SA 162 g of iPP-SA, 162 g of EP-amine, and 1 g of I-1076 were mixed in a 300-cm³ Brabender Plasticorder. The progress of the amine–anhydride condensation reaction was monitored by IR spectra (vide infra) of small aliquots of the melt. Intensive mixing at 60–80 rpm at reaction temperatures of 175–210 °C for 5–8 min was found to be necessary for the reaction. More severe reaction conditions (higher temperatures or longer reaction times) lead to degradation of the polyolefins. At the end of the reaction period the contents of the mixer were cooled and removed.

Blends. Solution Synthesis. The composition of the blend reflects the total amount of iPP and EP present: this includes the effect on the composition due to the addition of the compatibilizer. In a representative synthesis of a blend with 80% iPP and 20% EP with 5% of the graft compatibilizer, 94.8 g of PP-L, 22.9 g of EP-1, and 6.2 g of a graft compatibilizer of composition 65/35 iPP/EPDM (graft C, Table II) were dissolved in 1.5 L of refluxing xylene maintained under an atmosphere of N_2. The solution was poured into evaporating dishes which were greatly heated to maintain the xylene solution at its boiling point. Compositional fractionation of the blend by selective precipitation of iPP from the solution does not occur at these conditions. The solvent evaporated over a period of several hours to leave a residue of the polymer blend.

Blends. Melt Synthesis. In a representative synthesis of a blend with 80% iPP and 20% EP with 5% of the graft compatibilizer (blend Z-5 in Table V), 206.5 g of PP-L, 50 g of EP-1, and 13.5 g of graft compatibilizer of composition 65/35 iPP/EP (graft C, Table II) were melt blended with 1 g of I-1076 in a 300-cm³ Brabender Plasticorder. Intensive shear mixing for 4–6 min at temperatures of 180–195 °C was adequate. The blend was cooled and chopped into pieces 5 mm in diameter suitable for injection molding.

Characterization. Molecular Weight. Molecular weight measurements were made in 1,2,4-trichlorobenzene solution by a combination of a Waters 150C GPC with an on-line scattering KMX-6 Chromatix-Milton Roy. The laboratory procedures have been described.[27] Molecular weights are determined with reference to calibrated polystyrene standards. EP-amine, EPDM-amine, and iPP-SA need to be "capped" at the functional group prior to analysis since uncapped samples strongly absorb on the column packing through the functionality. This leads to preferential retention of the polymer on the column and large errors in the molecular weights. The amine and anhydride samples were capped by reaction with a 100-fold excess of acetic anhydride and 1-hexylamine, respectively, in a refluxing xylene solution for 3 h. These reactions form the corresponding EPDM-acetamide and iPP-succinimide. The polymer was isolated by repeatedly washing the reaction mixture with water followed by evaporation of the solvent.

Graft Polymer. Fractionation. Differential solvent extractions were performed in Kumagawa (Soxhlet) devices under nitrogen atmosphere. A small amount of (7–10 g) of the polymer was embedded as a thin film on a stainless steel screen (100 mesh) in a hot (160 °C) press. This sample was placed in a thimble and extracted with about 400 mL (containing 300 ppm of I-1076) of refluxing solvent for 24–36 h. At the end of this period the solvent containing the soluble polymer fraction was isolated and dried. The insoluble fraction in the extraction thimble was dried in situ and reextracted with a new solvent. Refluxing pentane, hexane, cyclohexane, heptane, isooctane, toluene, and xylene were used as a series of increasingly effective solvents with higher boiling points. The temperature of the solvent in the extraction thimble was monitored with a thermocouple near the sample. In all cases the temperature of the solvent in the thimble was significantly lower than the boiling point of that solvent: these differences are larger for higher boiling solvents such as xylene and toluene.

Dynamic Mechanical Thermal Analysis. The thermal analysis of the polymers was performed on a Polymer Labs DMTA dynamic mechanical thermal analyzer at 3 Hz. Each sample was a bar of about 1 g with dimensions $1 \times 4 \times 0.25$ cm. After mounting the samples were quenched to −85 °C and then heated at 2 °C/min up to 200 °C during the measurement. The elastic modulus, E', loss modulus, E'', and loss tangent, tan δ, were all measured once per degree Celsius.

Differential Scanning Calorimetry. DSC was measured using a Perkin-Elmer instrument for samples between −50 and +200 °C at a scanning rate of 10 °C/min. Graft polymer samples were molded into pads suitable for DSC and then slowly annealed at room temperature for 3–4 days prior to analysis. Samples were mounted, quenched to −100 °C, and then slowly heated to −50 °C. Spectra were usually run in duplicate.

Infrared Spectroscopy. Infrared spectra of the polymers were recorded for films between 0.17 and 0.35 mm thick using a Perkin-Elmer FTIR spectrometer. This was used to determine both the ethene content of the polymer using ASTM procedure D3900 and the composition (EP/iPP ratio) of the fractions separated by differential solvent fractionation according to the procedure described below. For each sample absorbances at 1155 and 722 cm^{-1} which are characteristic of propene (in EP or iPP) and ethene (in EP) residues, respectively, were measured. A calibration curve, made by blending known amounts of EP-1 and PP-L in the composition range of the polymer fractions, correlated the spectral data to the EP/iPP composition of the samples.

Electron Microscopy. The morphology of the blends was examined by scanning electron microscopy (SEM) and transmission electron microscopy (TEM). Compression- and injection-molded samples were cryogenically (−196 °C) microtomed to sections 50–100 μm thick with a Reichert-Jung FC-4 ultramicrotome. The imaging contrast for SEM was provided by dissolving the EP with hexane in an ultrasonic bath at ambient temperature. This created holes isomorphic with the EP domains in the section. We assume that the iPP matrix for the blends was unaffected by this extraction procedure and that all of the EP was extracted. Microtomed sections of the blends containing less than 70% iPP were fragile after the extraction procedure and were easily deformed during subsequent manipulation. This is a practical limitation on the composition of iPP/EP blends which can be analyzed by this procedure. Samples for SEM were carbon coated prior to imaging using a Robinson back-scattered electron detector. Thin sections of each sample for TEM were stained in the vapor space above a 1% aqueous solution of RuO_4 for several days. The metal oxide preferentially attacked the olefin of EPDM-amine, while the rest of the polyolefin was relatively unaffected. Thus micrographs of the sections showed darker images for the location of the EPDM-amine compared to the other polymers.

Image Analysis. Image analysis of SEM micrographs having a high contrast between the holes corresponding to the dispersed EP phase and the surrounding iPP matrix was used to determine the particle size and the area of the dispersed phase. SEM micrographs were scanned at a resolution of 200–300 dpi on an Apple laser scanner to create a digital dot matrix file. This was

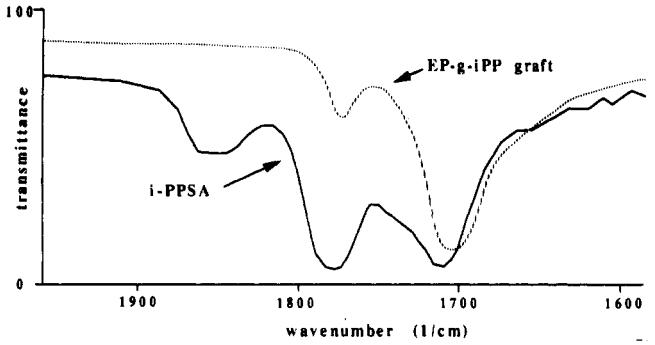

Figure 2. IR spectra of (i) iPP-SA and (ii) EP-*g*-iPP for the carbonyl region. Note the succinic anhydride absorptions in (i) and the succinimide absorptions for (ii).

analyzed by Image (Version 1.29), a software developed by Wayne Rasband (NIH), operating on an Apple Macintosh IIsi personal computer. The program differentiates between the images of the dispersed phase and the surrounding matrix according to the contrast between these features. Data for the area and diameter of the dispersed phase particles are generated by this analysis. Statistical analysis of the data is performed using Kaleidagraph 2.1 data analysis software. Typically, approximately 1000 particles from 5 to 6 micrographs were analyzed to obtain statistically significant results. Images which show a range of sizes for the dispersed particles have a practical limit in the accuracy of the image analysis procedure. SEM images are a compromise between low magnification which shows enough of the larger particles in a limited number of pictures and a high magnification which shows even the smallest particles. A measure of the accuracy of the analysis is the ratio of the combined area of the dispersed phase for all the images as a fraction of the total area of the images. Ideally,[28] this should be the same as the volume fraction of the dispersed phase in the blend. We have chosen the magnification of the SEM pictures to preserve this ratio, from the image analysis, within 10% of the value expected from the ratio of blend components. In view of other systematic errors in these analyses, efforts at further increasing the precision in these procedures do not lead to a corresponding increase in accuracy.

Mechanical Properties. The impact strength of the blends was measured using ASTM D256, Method A. Samples were injection molded at barrel temperatures of 190–210 °C into standard test bars on a Boy injection machine. For each blend five independent measurements were taken and the middle three are averaged for the final result reported here. The low-temperature measurements, between 0 and −45 °C, were obtained by cooling the samples in an insulated 2-propanol bath, cooled with periodic addition of dry ice. The sample was maintained at the desired temperature for at least 20 min before it was moved and broken at the impact tester. We assume that in the 7–10 s between removal of the sample from the bath to the completion of the test no significant warming of the sample takes place.

The flexural modulus according to ASTM D790, Method A, and tensile strength according to ASTM D638 were measured on 3-mm-thick injection-molded test bars of the blends.

Results and Discussion

Grafting Reaction. The first thing that was important to determine about the products of this reaction was that the grafting reaction did indeed occur between the two reactants. This was done by a variety of techniques that observe changes on grafting at different portions of the molecule and reflect the structure of the product at different length scales.

Infrared Spectroscopy. The formation of the graft polymer occurs by the condensation of a primary amine group with a succinic anhydride group to form a succinimide by elimination of water (**1b**, Figure 1). This change in the chemical environment of the carbonyl groups is diagnostic for this reaction and is easily observed in the IR spectra of the polymers. The IR spectrum of the iPP-SA (Figure 2) has a peak in the carbonyl region at 1780 cm^{-1} due to the anhydride.[26] Figure 2 also shows the spectrum measured over the same frequency range for graft A which is the product of reacting 30% iPP-SA with 70% EP-amine. The composition of the reaction mixture was adjusted so that the ratio of amine groups to anhydride groups was 1.2 to ensure complete conversion of the anhydride to imide. The anhydride peak at 1840 cm^{-1} is significantly reduced in the reaction product, indicating a lower concentration in the graft polymer. More important, a new absorbance at 1710 cm^{-1} which is typical of imides[26] appears in the reaction product. The assignment of these spectral features for the graft polymer is supported by their similarity to the corresponding absorbances for the imide formed from the reaction of 1-dodecylamine with iPP-SA. Figure 2 shows that the extent of conversion of the amine and anhydride to the imide is essentially complete to the limit allowed by the composition. A more quantitative estimate of the concentration of imide and hence the extent of reaction was not possible because of the absence of values for the extinction coefficient for the 1710-cm^{-1} absorbance for the imide in a nonpolar, polymeric environment. Infrared spectroscopy is sensitive to the formation of the imide groups: it does not indicate if "true" graft polymers are made. It is possible to have similar spectral changes from the reaction of EP-amine with oligomeric succinic anhydride containing material in iPP-SA. The existence of true graft polymers is proven by other techniques which look at the larger scale structure of the polymers.

Molecular Weight. One effect of grafting two or more polymer chains together should be that the molecular weight of the product is higher than those of the reactants. Further, both iPP-SA and EP-amine have a distribution of molecular weights with an approximately uniform concentration of reactive functionality. The probability of a polymer chain undergoing the grafting imidization reaction thus rapidly increases with molecular weight. The largest increases in the molecular weight should be most apparent for the higher molecular weight segments. These changes in molecular weight on grafting are often difficult to observe in a size-exclusion chromatogram (especially compared with the changes seen in block polymers) since the hydrodynamic volume of the branched chains often does not increase as rapidly as the molecular weight.[29] However, for the polymers graft A–C described here we did see a significant increase in the molecular weight compared to either of the starting materials EP-amine or iPP-SA. This is shown in the results summarized in Table II. The number-average molecular weight of the products in all three cases was intermediate between those of the two reactants. This is the average contribution of the low molecular weight fraction of either polymer which does not undergo the grafting reaction since it is not functionalized. The weight, z, and $z + 1$ averages for all of the molecular weight distributions were all much higher than either of the parent polymers. This was especially true for the $z + 1$ average of all the graft polymers and for all of the molecular weights of graft A. Further, all of the molecular weight distributions of the graft products were significantly broader than for the reactants. These changes are consistent with the model of the random imidization reaction where the probability of grafting to form higher molecular weight grafts increases rapidly with the molecular weight of the reactants.

The molecular weight data indicate the formation of true graft polymers but does not estimate the extent of the grafting reaction and consequently the number of iPP-SA grafts on the EP backbone. A reasonable estimate based on the increase of the molecular weight of the grafts indicates that between 3 and 10 iPP grafts per EP backbone

Table III
Results for Differential Solvent Fractionation of EP-*g*-iPP Polymers (A–C) and an EP/PP Blend (D)[a]

		differential solvent fractionation: solubility			compositional analysis of fractions by IR		
sample	wt of sample (g)	solvent	wt of fraction (g)	total wt of fractions (g)	EP wt % of fraction	wt of EP fraction (g)	total wt of EP in sample (g)
A	5.814	pentane	0.803	5.748 (98% of sample)	92.4	0.742	3.870 (95% of EP from synthesis)
		hexane	0.889		62.5	0.556	
		cyclohexane	2.782		77.9	2.167	
		isooctane	0.659		49.1	0.324	
		toluene	0.305		21.4	0.065	
		xylene	0.120		13.3	0.016	
		insoluble	0.190				
B	7.174	pentane	0.432	7.095 (98% of sample)	79.7	0.344	3.528 (98% of EP from synthesis)
		hexane	0.238		63.4	0.150	
		cyclohexane	1.041		75.6	0.787	
		isooctane	3.421		55.2	1.888	
		toluene	1.543		21.2	0.327	
		xylene	0.328		9.8	0.032	
		insoluble	0.101				
C	6.712	pentane	0.091	6.781 (101% of sample)	68.8	0.062	2.276 (97% of EP from synthesis)
		hexane	0.295		65.0	0.192	
		cyclohexane	0.262		78.3	0.205	
		isooctane	0.888		54.0	0.479	
		toluene	4.043		25.9	1.047	
		xylene	1.202		24.3	0.291	
		insoluble	0				
D	7.241	pentane	2.099	7.316 (101% of sample)	96.5	2.026	2.238 (103% of EP from synthesis)
		hexane	0.181		76.7	0.139	
		heptane	0.076		48.6	0.037	
		toluene	0.398		9.1	0.036	
		xylene	4.562		0	0.0	
		insoluble	0				

[a] Data are for the amount and composition of the soluble polymer in each solvent.

are formed in all three cases. A more quantitative estimate is obtained from the solvent fractionation results shown below.

Differential Solvent Fractionation. Solvent fractionation of the graft polymers A–C with several refluxing solvents of slowly increasing solubility parameters and boiling point provides several fractions different in iPP-SA/EP-amine ratio. This is direct evidence for the formation of graft polymers of iPP-SA and EP-amine and also provides an estimate for the number of iPP-SA grafts on the EP backbone in the graft polymers A–C.

The reactant polymers, EP-amine and iPP-SA, are soluble in refluxing pentane and xylene, respectively. These are the extremes of the set of solvents used for the differential solvent extraction. The difference in the solubility behavior arises from the amorphous nature of the EP-amine and the crystalline habit of iPP-SA. Mixture of these polymers, in the absence of a grafting reaction, should yield a "clean" separation into fractions of EP-amine and iPP-SA soluble in these two solvents with no other fractions soluble in intermediate solvents. Since blends of these two polymers readily react, the fractionation data are modeled by the blend D which is a 30/70 mixture of EP-amine and PP-L. No grafting reaction can occur between these polymers, and the fractionation results are shown in Figure 3 and Table III. The pentane-soluble fraction contained essentially all of the EP-amine, and nearly all of the PP-L was in the xylene-soluble fraction. Only a very minor part of either of the polymers ended up in the intermediate fractions, and there was essentially no contamination of either the main PP-L or the EP fraction with the other component.

Graft polymers formed by the reaction of EP-amine and iPP-SA are expected to have solubilities intermediate between the constituent polymers. Thus, if grafting of iPP-SA to EP-amine does occur, some of the polymer will be soluble in the intermediate fractions. Further, the extent of solubility of the graft polymer in these fractions is an indication of the extent of the grafting reaction. In

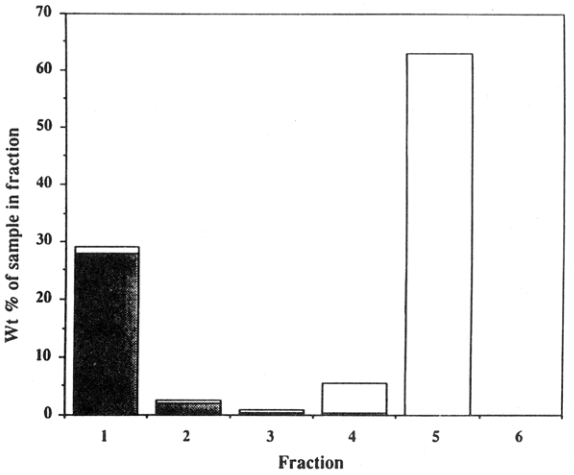

Figure 3. Separation of fractions by differential solvent extraction and their analysis for composition (EP/PP ratio) of a blend of 30/70 EP/iPP polymers. Fractions are as follows: 1, pentane soluble at 39 °C; 2, hexane soluble at 57 °C; 3, heptane soluble at 89 °C; 4, toluene soluble at 94 °C; 5, xylene soluble at 113 °C; 6, insoluble gel. For each fraction the total height of each bar is the weight percent of the sample. Composition of the fractions (EP/PP ratio, by IR) is shown by the relative heights of the shaded (EP) and the clear (iPP) regions.

contrast to the fractionation data for the blend of nonfunctional polymers, the fractionation results from grafts A–C were dominated by the fractions of intermediate solubility, as shown in parts A–C of Figure 4 as well as Table III. The compositions (EP/iPP ratio from IR) of the fractions in any one solvent isolated in all three cases were nearly the same; only the amounts of each fraction changed with the amounts of iPP-SA and EP-amine used to make the graft polymers. Moreover, in all cases both the pentane and xylene fractions contain a significant amount of iPP and EP, respectively. This is different than the results with the blend and indicates the existence of graft polymers. In each case there was a small fraction of xylene-insoluble material, which indicates that some

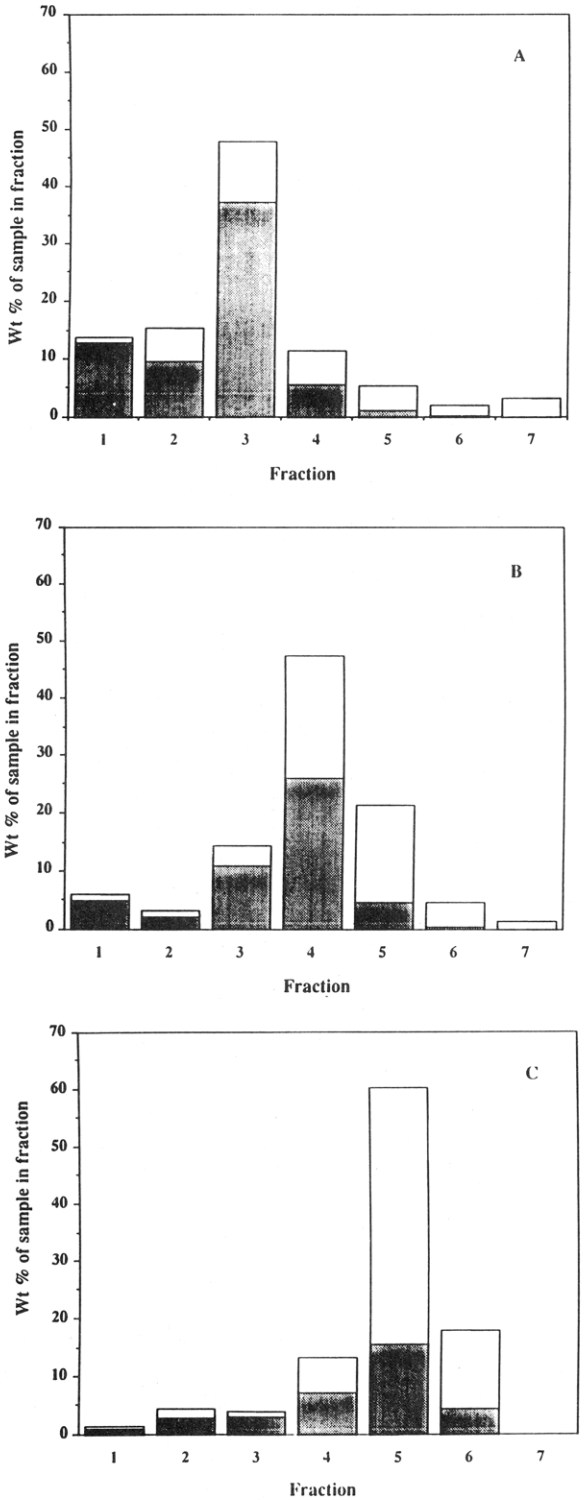

Figure 4. Separation of fractions by differential solvent extraction and their analysis for composition (EP/PP ratio) of EP-*g*-iPP polymers. EP-*g*-iPP polymers are the following: (A) graft A, (B) graft B, and (C) graft C. Fractions are as follows: 1, pentane soluble at 39 °C; 2, hexane soluble at 57 °C; 3, cyclohexane soluble at 72 °C; 4, isooctane soluble at 88 °C; 5, toluene soluble at 94 °C; 6, xylene soluble at 113 °C; 7, insoluble gel. For each fraction the total height of each bar is the weight percent of the sample. Composition of the fractions (EP/PP ratio, by IR) is shown by the relative heights of the shaded (EP) and the clear (iPP) regions.

cross-linked gel was formed. It is possible that iPP-SA contains a significant amount of multifunctional polymers, which would lead to such gel formation. But this was only a very small part of the product of these reactions.

Our results indicate that solubility is principally a function of the average composition of the graft since polymers with a higher proportion of iPP-SA will be preferentially soluble in better solvents at a higher reflux temperature. However, both EP-amine and iPP-SA contain a broad distribution of molecular weights. The expected random imidization reactions should produce individual graft molecules with a distribution of compositions about the mean. Thus, for example, the reaction of a low molecular weight EP-amine molecule with a high molecular weight iPP-SA molecule should produce a graft molecule with a higher proportion of iPP-SA than the mean composition for the blend. This statistical variation in the composition of molecules in the graft polymer accounts for the breadth of the fractionation distribution.

The fractionation data can be used to estimate the number of iPP-SA grafts on the EP-amine backbone for the graft polymers A–C. This can be determined from the amount and composition (iPP-SA/EP-amine ratio) of the various fractions using the models of Stejskal et al.[30,31] The amount of the fraction is determined gravimetrically, while the composition of the fraction is determined from the ratio of IR absorbances at 1055 and 722 cm^{-1} as shown in the Experimental Section. This model predicts all of the parameters and their statistical distributions relevant to the grafting process for a random grafting reaction. Two parameters are required for the complete solution of this statistical analysis. These are (i) the molecular weight distributions of the reactants EP-amine and iPP-SA and (ii) a characteristic of the graft polymer related to the extent of grafting such as the average number of grafts per backbone or the fraction of backbone having attached grafts.

A convincing way of comparing experimental results to the predictions of this model is to observe the cumulative distribution of composition, $S(x)$. $S(x)$ is defined as the fraction of the whole graft copolymer product that has a composition x (fraction of EP-amine) or less. The derivation of $S(x)$ from the Stejskal model is shown in the appendix. The fractionation data for the graft polymers are a direct experimental observation for this theoretical parameter. The comparison of these two parameters is shown for these three graft polymers A–C in parts a–c of Figure 5, respectively. The match between the Stejskal model and the experimental data indicates that the grafting for each graft polymer is essentially complete to the limit of the composition. Further, from the molecular weight distributions found in Table II, the average number of iPP-SA grafts per EP-amine backbone can be calculated as 0.788 in graft A, 1.84 in graft B, and 3.41 in graft C. Clearly these fractionation results are very useful in characterizing the product of a grafting reaction.

Graft Morphology. Thermal Analysis. Modifications of the thermal behavior of polymer systems, particularly in the temperatures and breadths of various transitions of state, are often used to show changes in their morphology and miscibility. Such effects have been seen in the graft polymers made by the method described herein when they are compared to simple blends of EP and iPP. Here both DSC and DMTA results from grafts A–C are compared with those of blend D, where no grafting could have occurred since the EP contained no functionality. The DSC results listed in Table IV show that the melting point of the iPP-SA was lowered in the grafts, with a corresponding lowering in its degree of crystallinity as indicated by the lower enthalpy of melting. This can be explained by assuming that part of the iPP-SA was found in an interfacial region (or interphase) in the graft products where it is intimately mixed with some of the EP-amine. Crystallization of this material is expected to be slow and lead to an imperfect crystal structure. The DMTA data which are shown in Table IV and Figure 6 support this model for the structure of the graft polymer.

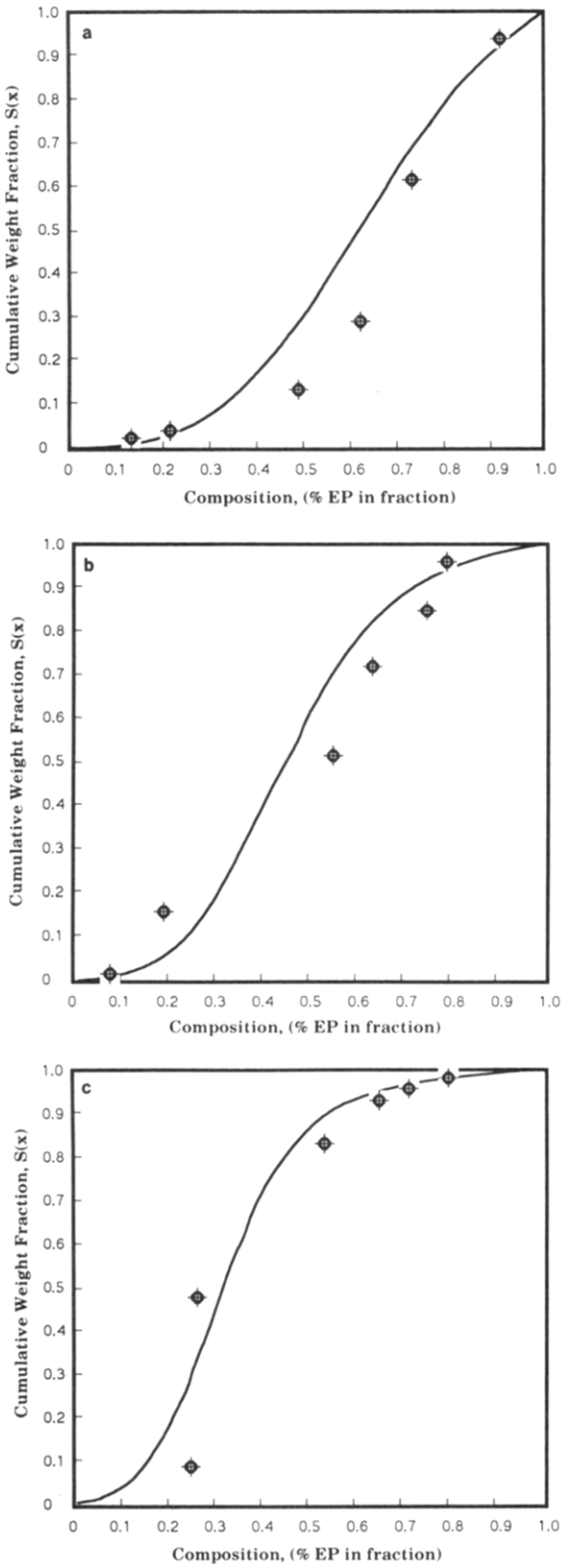

Figure 5. Predicted (continuous line) function $S(x)$ versus measured compositional (O) fractions for the EP-*g*-iPP graft polymers: (a) graft A, (b) graft B, and (c) graft C.

This shows that the glass transition behavior of the grafts is also different from that of a blend. The glass transition for the EP phase tends to move to higher temperature, while that of the iPP moved to lower temperature. This can again be explained by an increase in the mixing at a molecular scale between the components, perhaps in an interfacial region. This evidence from the thermal analysis suggests a large interfacial area for the domains of EP-amine and iPP-SA. The morphology of the graft polymers as well as a quantitative estimate of the size of the domains

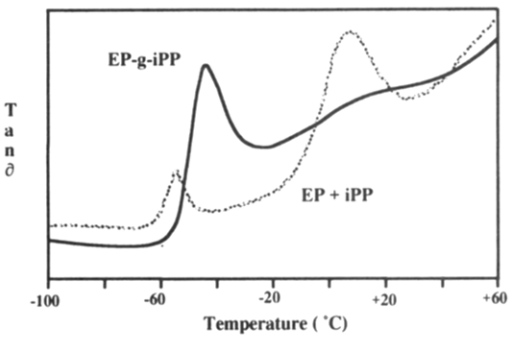

Figure 6. Dynamic mechanical thermal analysis for graft C (solid line) and blend D (broken line).

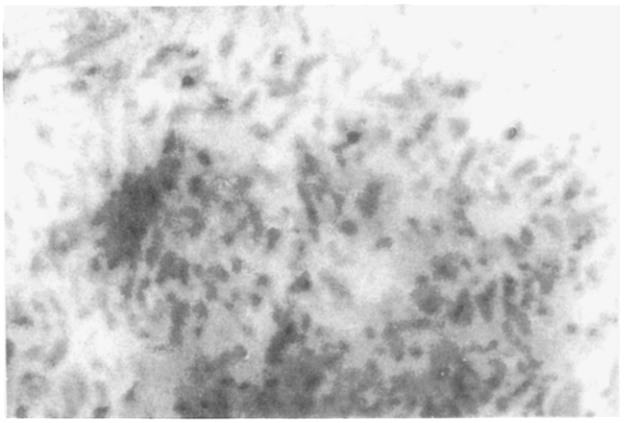

Figure 7. TEM micrograph for the RuO_4-stained graft C*. The dark regions are domains of EPDM-amine.

Table IV
Results of Thermal Analysis for Grafts A–C and Blend D

	DSC results (iPP melting)			DMTA results	
sample	T_m (°C)	onset melting (°C)	ΔH_f (J/g) for iPP	T_g (°C) for EP	T_g (°C) for iPP
A	147.7	109.5	240.3	−43	broad at +10
B	151.5	135.8	75.2	−44	not obsd
C	151.6	140.8	57.5	−50	broad at +6
D	161.7	156.5	206.1	−50	+10

was obtained from the transition electron microscopy shown in the next section.

Microscopy of Pure Grafts. The morphology of graft C* is shown in Figure 7. The dark regions are the domains of the EPDM-amine which have selectively stained by exposure to RuO_4. The sample consists of domains of EPDM-amine and iPP-SA which are microphase separated with a characteristic scale of a few nanometers. This is consistent with both the thermal analysis data shown above and the molecular weight of the reactive components. The domains of EPDM-amine in graft C* appear ellipsoidal of dimension 10 × 40 nm rather than spherical. The reasons for this distortion are unclear. We assume that the morphology of EP-amine/iPP-SA grafts are similar. Since the morphology of these graft polymers has not yet been investigated in detail, we are unable to indicate whether this is expected from a graft or if this should be a particular feature of these polymers.

The microscopy and the thermal data, considered in conjunction, fully support and define a microphase-separated morphology for the graft polymers. This is consistent with the molecular structure which has been elucidated by a variety of probes sensitive to different features of the graft polymer.

Table V
Composition of Blends of Isotactic Polypropylene, Ethylene–Propylene Copolymer and Graft Polymers

	polypropylene		EP-1	graft	
blend	type	amount (g)	amount (g)	type	amount
X-0	PP-H	80	20	C	0
X-2		78.3	19.6	C	2
X-5		76.4	18.6	C	5
X-10		72.9	17.1	C	10
X-0*	PP-H	80	20	C*	0
X-2*		78.3	19.6	C*	2
X-5*		76.4	18.6	C*	5
X-10*		72.9	17.1	C*	10
Y-0	PP-H	85	15	C	0
Y-2		83.5	14.4	C	2
Y-5		81.4	13.6	C	5
Y-10		77.9	12.1	C	10
Z-0	PP-L	80	20	C	0
Z-2		78.3	19.6	C	2
Z-5		76.4	18.6	C	5
Z-10		72.9	17.1	C	10

Compatibilized Blends. A series of blends of containing iPP and EP were made using the graft polymer C as a compatibilizer. The composition of the blends are shown in Table V, and the blends contain at most 20% of EP. Two different iPP, PP-L and PP-H, which differ principally in their molecular weights, were used in the blends as indicated in Tables I and V. Differences in the molecular weight of the polypropylene matrix phase are manifest in significant differences in the stability of the blend morphology and the impact strength of the compatibilized blends. We recognize that the morphology obtained during intensive shear blending may not be thermodynamically the most stable one. Blends were heated to above the melting point of the iPP (163 °C) for an extended period of time in order to observe the formation of the thermodynamically stable morphologies. Another series of blends, the X* series, was made using graft C* as the compatibilizer. The main difference between C and C* is that the latter contains some unsaturation since it uses EPDM-amine as the grafting backbone. This was important for the experiments which attempted to locate the compatibilizer as described below.

Microscopy of Compatibilized Blends. Thin sections of the iPP–EP blends were prepared for SEM as described above. Images of these sections were analyzed, and for each particle the area, the lengths of the major axes, and the aspect ratio of the domain were measured. The average and the standard deviation of these parameters for all of the particles were calculated. In addition, the sum of the area of the EP particles for each blend was compared to the area of the micrograph being analyzed. This is shown in parts A and B of Table VI for blends with low (PP-L, series X) and high (PP-H, series Z) molecular weight iPP, respectively. All of the blends contain a total of 80% of iPP, the balance being EP. Each table shows blends with 0%, 2%, 5%, and 10% of the graft polymer C, and for each different concentration of the graft polymer the morphology of the dispersed EP phase has been determined for two different thermal histories. The first row shows the data for the blends as they are made, while the second row shows data for the same blend after it has been annealed at 180 °C for 2 h. The annealing temperature is above the melting point of the iPP matrix (164 °C). We expect that the annealed samples, compared to the samples as blended, are closer to the thermodynamically stable morphology. In all micrographs the EP particles are elliptically distorted in the injection-molding direction. In the unannealed blends, with either PP-L or PP-H as the iPP, the effect of the addition of graft C was to reduce the size of the dispersed EP phase domains and to make them more spherical (Figure 8). These two effects are correlated since distortion of the EP particles probably occurs due to the shear stress of injection, and it has been shown[33] that smaller particles are less easily deformed than large ones. Larger amounts of added compatibilizer show correspondingly larger morphological effects. Comparison of the data for PP-H (X series) and PP-L (Z series) indicates that these morphological effects are more pronounced in the blends with lower molecular weight iPP. This is principally because the particles of the dispersed EP are larger for these blends in the absence of the graft polymer. We believe that this poorer dispersion of the EP arises from a much lower molecular weight of the iPP compared to the EP. This translates to a corresponding disparity in the melt viscosity of these polymers at the blending temperatures and a poorer dispersion or larger domains of the EP.[14,15]

The other effect of the addition of graft C was to stabilize the morphology of the blend during annealing above the melting temperature of the iPP. The blends without the compatibilizer showed a growth in the area of the EP domains by a factor of 4–10. The degree of increase was less for the blends with the graft, and there was essentially no growth for the blends with 5% or 10% compatibilizer. These morphological changes are shown in the micrographs presented in Figure 9 for series X. The change in the dimensions of the dispersed EP phase is less for the PP-H matrix than for the PP-L. This can be seen in the data in Table VI. Further, the EP particles all became more spherical during the annealing (that is, the average aspect ratio became closer to 1), even for the blends with 10% graft that showed no growth in domain size. These experiments show an enhanced stability of the dispersed morphology for blends with the graft polymer.

There are two mutually nonexclusive explanations for this. The first is that the presence of the graft polymer leads to a reduction in the interfacial tension between the phases which would reduce the driving force for phase separation. Thus the addition of graft polymer induces a thermodynamically stable blend morphology. The second is that the presence of the multiarmed graft polymer at the EP domain–iPP matrix interface retards the growth of the dispersed phase by a steric stabilization mechanism. In a melt-mixed, multiphase blend the ultimate particle size is determined by the competition between the breakup of the particles due to shear forces ("Rayleigh instability") and their growth due to coalescence. This phenomenon has been described by Grace,[14] and coalescence has been studied by Elmendorp and van der Vegt.[15] Thus the presence of compatibilizers at the interface can not only permit smaller droplets to form by means of the breakup mechanism because interfacial tension is lowered but also may reduce or prevent the growth of particles by steric stabilization. The data do not allow us to judge the relative importance of either mechanism during annealing of the blends. We note that even in the blends containing the largest amount of the graft polymer the interfacial tension has apparently not been completely eliminated. Thus the particles of the dispersed phase even in these blends tend to reduce interfacial free energy by becoming rounder during annealing to reduce surface area. Further study in this area to determine more about the mechanisms of the growth of dispersed domains and how compatibilizers slow it down is required to differentiate between these mechanisms.

Implicit in either mechanism for the stabilization of the morphology of the compatibilized blends, and, in fact, in the belief that the graft polymers will act as compatibilizers, is their localization at the interface between the phases. This has generally been assumed in work on compatibi-

Table VI
Morphologies of Blends X and Z before and after Thermal Annealing

		EP particle						
		area (μm^2)		major axis (μm)		aspect ratio		
blend	condition	mean	stand dev	mean	stand dev	mean	stand dev	no. of particles
				Blends X				
X-0	before	0.107	0.07	0.24	0.09	0.56	0.14	714
X-0	after	0.995	1.05	0.58	0.31	0.78	0.21	1159
X-2	before	0.142	0.16	0.23	0.13	0.70	0.18	1095
X-2	after	1.11	0.975	0.65	0.31	0.83	0.18	1231
X-5	before	0.043	0.044	0.13	0.12	0.71	0.20	1044
X-5	after	0.057	0.032	0.15	0.29	0.85	0.27	879
X-10	before	0.032	0.10	0.11	0.11	0.61	0.17	1058
X-10	after	0.030	0.09	0.10	0.12	0.86	0.13	1121
				Blends Z				
Z-0	before	2.91	9.26	0.95	1.00	0.61	0.19	991
Z-0	after	10.47	24.6	2.17	1.26	0.81	0.15	988
Z-2	before	1.87	5.57	0.89	0.77	0.57	0.18	991
Z-2	after	4.38	6.54	1.63	0.79	0.74	0.12	961
Z-5	before	0.52	0.92	0.42	0.29	0.69	0.22	976
Z-5	after	1.02	0.84	0.64	0.37	0.86	0.29	989
Z-10	before	0.55	1.12	0.43	0.31	0.75	0.20	944
Z-10	after	0.64	0.93	0.40	0.27	0.85	0.13	1041

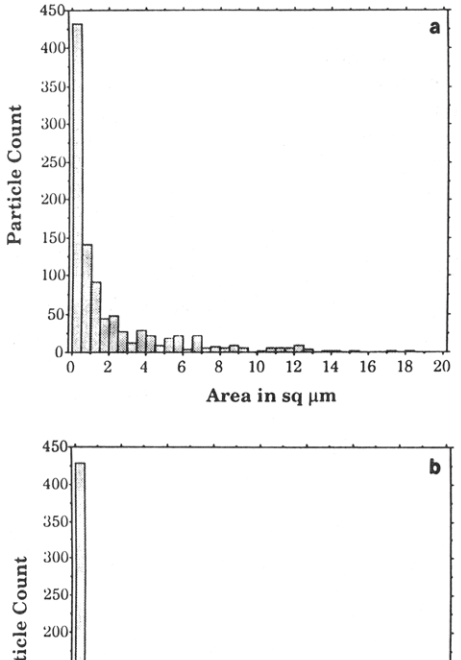

Figure 8. Particle size distribution for the dispersed EP phase for the blends Z-0 (a) before and (b) after thermal annealing. Particle sizes are expressed as the area of the particle in square microns.

lization but has only been demonstrated by Fayt et al. using differential staining.[10] The utility of the blends of the X* series was to be able to observe the image of the graft polymers by utilizing the unsaturation in the backbones of the C* molecules. Thin sections of each of the blends in this series were stained with RuO_4 and then imaged by TEM. Since all of the other components are completely saturated, they are less affected by the RuO_4 which strongly attacks olefinic unsaturation. Thus a strong contrast between C* and the other polymers is to be expected. This is shown for blends containing 0% (Figure 10a), 2% (Figure 10b), 5% (Figure 10c), and 10% (Figure 10d) of the graft polymer C*. In all the blends the EP domains can be seen as slightly dark domains because the EP absorbed more of the stain than the iPP. This was true even in the blend without graft polymer (X-0*, Figure 10a). However, in the blends containing the graft polymer a dark band was seen around the dispersed EP domains. In this progression of micrographs this dark band became better defined and more continuous with increasing amounts of the graft polymer. It is most pronounced for X-10*, which contains the largest amount of the graft polymer. We believe that this dark band defines the location of the graft polymer in these polymer blends to be at the interface of the incompatible polymers. The thickness of this layer varies somewhat in the image, but it is on the order of 20 nm. This is a reasonable size for the graft polymer of the molecular weights shown above. The fact that at least part of the graft polymer has been shown to be at the surface of the domains confirms the behavior expected and also helps in the explanation of both the reduction and stabilization of domain sizes. It should also be pointed out that the interfacial activity of these polymers is a confirmation that they are indeed graft polymers that have covalently bound EP and iPP sections, in agreement with all of the results cited above.

Mechanical Properties. The main practical interest in compatibilization and its potential to control phase domain sizes and shapes is due to the effect this has on properties, particularly those in the area of mechanical failure.[32] A convenient measure of such a property is the notched Izod (NI) impact strength of the blend. The effect that graft C had on the NI impact strength of iPP/EP blends is shown in parts a–c of Figure 11 for the X–Z series, respectively. The composition of these blends is shown in Table V. These data show variation in the NI impact strength at a range of temperatures from −40 to +25 °C for blends containing 0%, 2%, 5%, and 10% of the graft C.

The first thing to note is the overall difference in the absolute values of impact strength between the series. Higher NI impact strengths are both a function of the higher molecular weight of the iPP matrix (X vs Z) and the larger amount of rubber phase volume (X vs Y). Within each series the addition of the compatibilizer increased the impact strength. These increases were larger for greater amounts of the graft C and persisted throughout the temperature range of the experiments. The magnitude of the increase was also dependent on the nature of the blend; thus the changes are most prominent for blend Z.

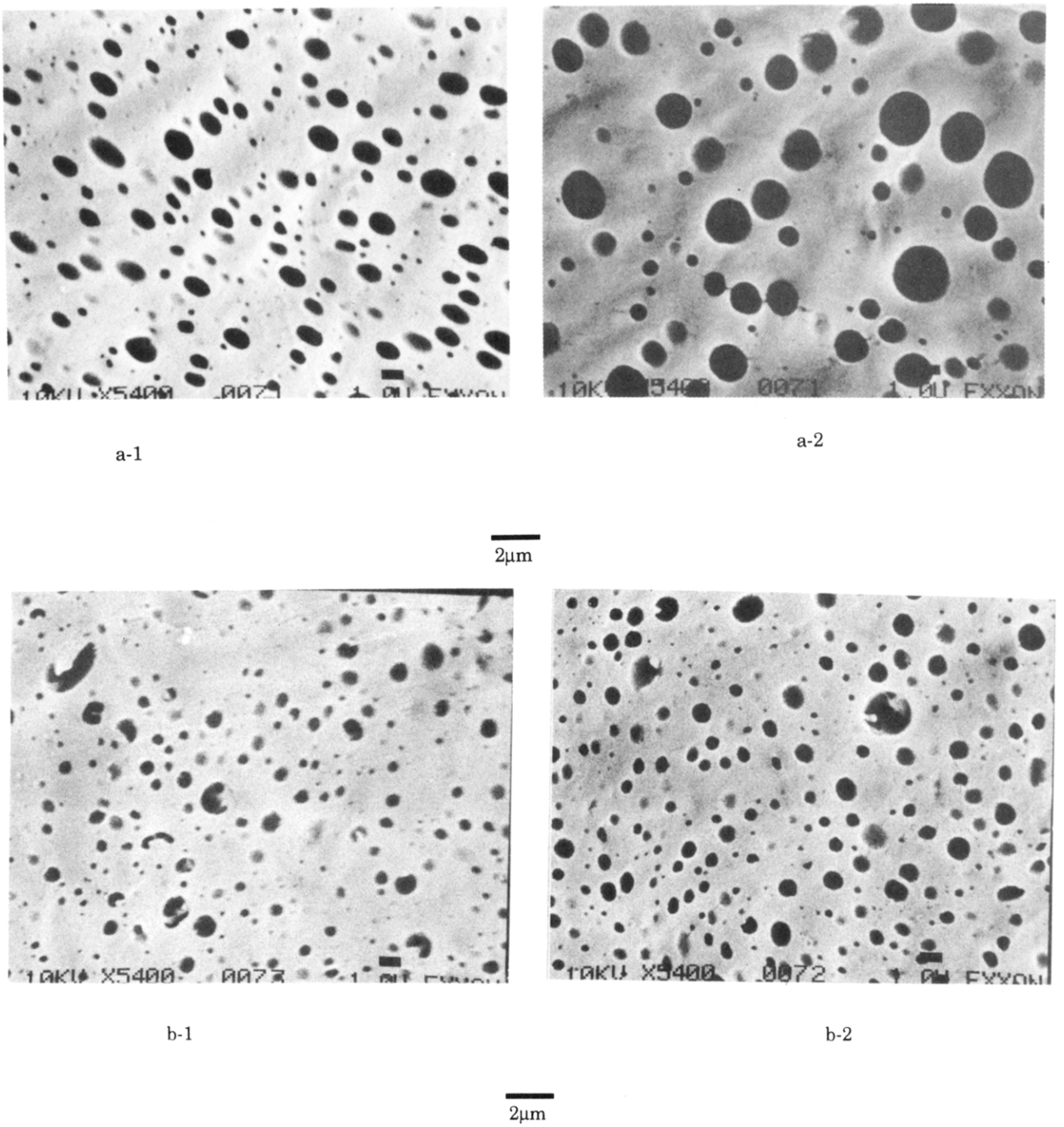

Figure 9. SEM micrograph for the hexane-extracted sections of the blends X-0 before (a-1) and after (a-2) thermal annealing. Similar micrographs for X-5 ((b-1) before annealing and (b-2) after annealing) are also shown.

Irrespective of either the amount of the compatibilizer or the composition of the blend, the variation of NI with temperature had the same characteristics. They all showed a nearly constant value of Izod strength at the higher temperatures (at least above 0 °C); then a significant drop in toughness below some temperature (usually between −10 to −30 °C), followed in some cases by another region of constant impact strength at a much lower value. At the higher temperatures these blends were ductile, and in the lower constant value region they were brittle. The transition point between these two regions is the ductile–brittle transition temperature, which defines a lower limit for the use of these blends in many applications. Brittle blends have low impact strength and are likely to fail easily. It is important to note that the addition of the compatibilizers reduced this transition temperature by as much as 20 °C for those with 10% graft. This indicates that these materials will have a greater utility over a correspondingly greater lower temperature range.[33]

An enhancement in properties is of interest only if it is not accompanied by a loss of some other important property of the blend. Of particular concern for such polymer blends is the stiffness of the blend, since most means of increasing the impact strength also reduce stiffness. That this was not the case for the blends studied here is shown in Figure 12, where the Young's modulus is plotted along with room temperature Izod impact strength as a function of percent added graft for the Y series. It is clear that the enhancement in toughness described above and shown in Figure 11a–c did not have a corresponding loss of stiffness but that it was essentially unaffected by the compatibilizer. Since this property depends mainly on the fraction of the low modulus component (EP rubber) which has been intentionally held constant for these blend

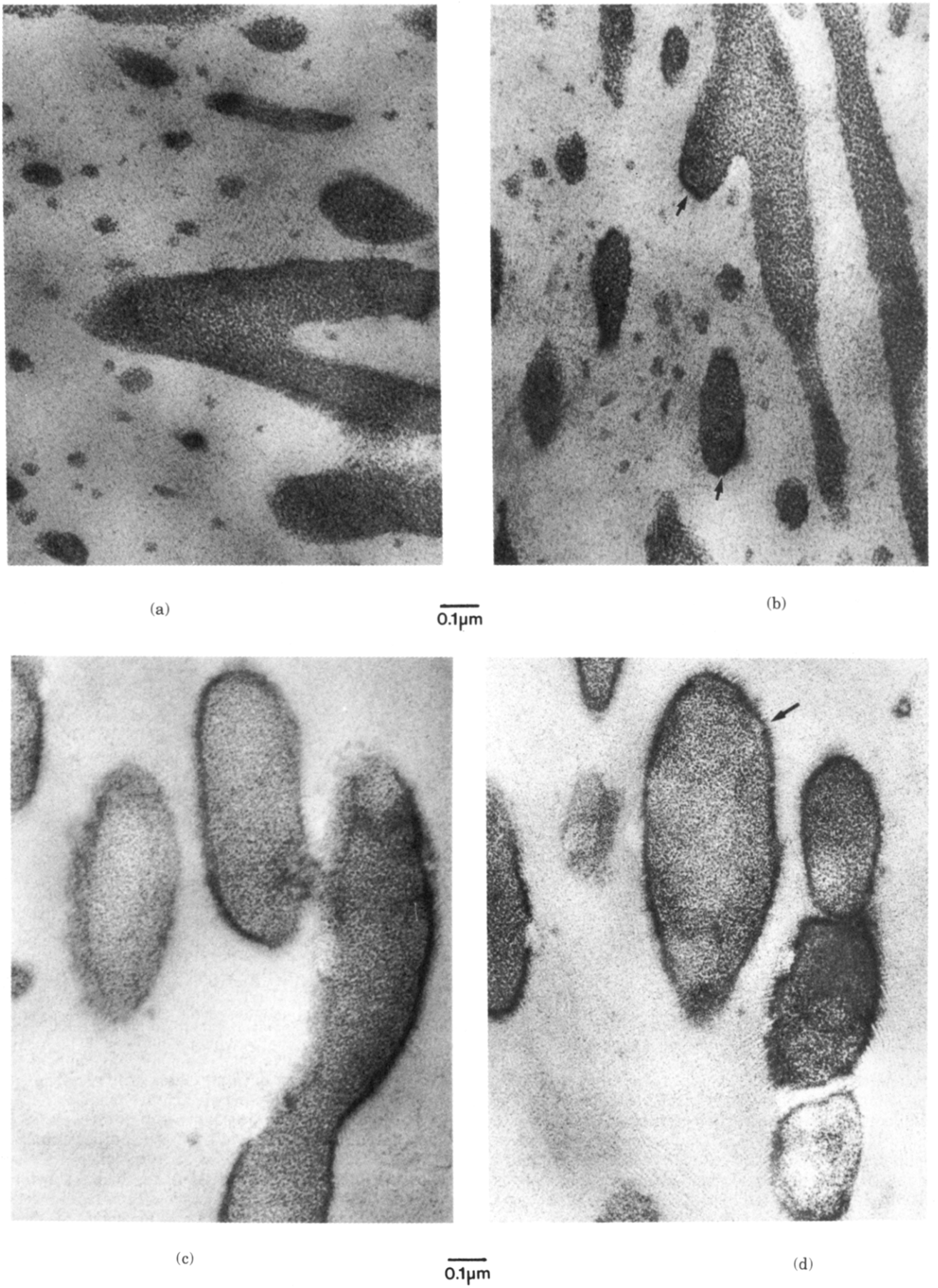

Figure 10. TEM micrographs for RuO_4-stained sections of blend (a) X-0*, (b) X-2*, (c) X-5*, and (d) X-10*. The dark periphery of the dispersed EP particles is the probable location of graft C*.

compositions, this was not unexpected.

The improvement in impact strength of the blend with no apparent loss of stiffness leads to several potential uses for these graft polymers. For instance, the extrusion rate of a blend such as the ones we have described is mostly a function of the melt viscosity of the matrix iPP. Thus,

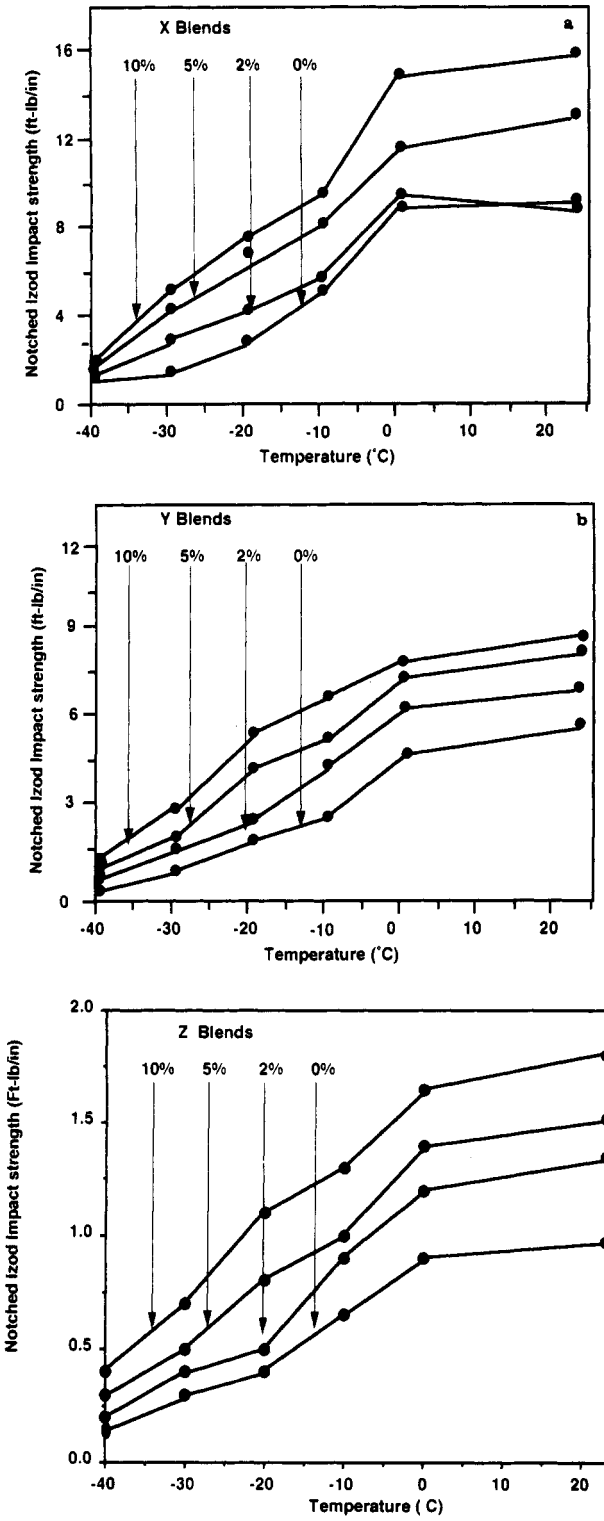

Figure 11. Notched Izod impact strength as a function of temperature and the amount of the graft polymer C for the blends (a) X, (b) Y, and (c) Z.

for iPP/EP blends the use of lower molecular weight iPP results in higher extrusion rates. In uncompatibilized blends this also leads to lower impact strength. An advantage of the compatibilizers described in this paper is the ability to use low molecular weight iPP as the blend matrix and still maintain good impact properties. This can be seen in Figure 11a–c, where the PP-L, with a melt flow rate 30 times larger than PP-H, showed comparable impact value in blends on the addition of the compatibilizer. Clearly the use of such graft copolymer compatibilizers increases the options available to the materials designer in achieving a suitable balance of relevant properties.

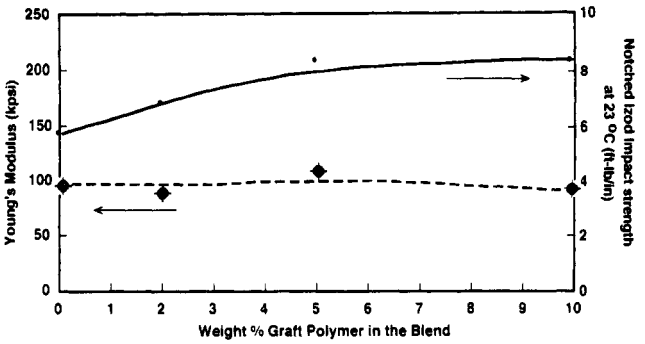

Figure 12. Room temperature Young's modulus and notched Izod impact strength vs amount of graft polymer C for Y blends.

Conclusions

The addition of a minor amount of a suitable block polymers to blends of incompatible polymers leads to a very efficient compatibilization. This is manifested in changes in morphology and mechanical properties (e.g., impact strength). However, except for a few notable examples, a block polymer compatibilizer for two polymers chosen at random is difficult because these compatibilizers cannot be synthesized. In practice most blends are compatibilized by the addition of a minor amount of a graft polymer (either preformed or formed in situ). Graft polymers are believed to function as compatibilizers by a mechanism similar to that of block polymers. However, there is very little consistent, complete, and convincing evidence about the synthesis, structure, effectiveness, and location of the graft polymers in a blend. Our work answers these questions for a model system of a blend of iPP and EP polymers. This work is a comprehensive account of the synthesis, characterization, and efficacy of a consistent set of EP-*g*-iPP graft polymers as compatibilizers of the incompatible polymer blend EP + iPP. This is the first example of such a comprehensive treatment of graft polymers which act as compatibilizers. It is expected that other graft polymeric compatibilizers behave in an analogous fashion.

It has been shown that a graft copolymer with an EP backbone and iPP pendant arms can be made with high grafting efficiency by the reaction of an amine EP with succinic anhydride containing iPP. These novel graft polymers are characterized at various molecular scales by a variety of experimental techniques. A detailed analysis of the fractionation data permits a quantitative description of the distribution of graft arms among the backbones. These polymers are compatibilizers for iPP/EP blends. This is shown by changes in morphology and mechanical properties. These changes in morphology are manifest in improvement in the impact strength without loss of stiffness. The cause of the particle size reduction is still unclear. This could be either due to a lowering of interfacial tension or due to a steric stabilization mechanism from the presence of the graft arms protruding from the particle surface. These graft polymers are located at the interface of the incompatible polymers in the blend.

Acknowledgment. This study and results are the outcome of a multidisciplinary approach to understanding this system. We thank Dr. L. Wheeler and Mr. J. Haberman for molecular weight determinations by SEC, Mr. L. Ban for microscopy of the polymers, and Mr. T. Pugel for some of the mechanical testing. We thank Mr. F. T. Morrar for the synthesis of the amine-functionalized EP polymers as well as the blend evaluations. We are grateful to Dr. E. N. Kresge, Dr. D. N. Schulz, and Dr. M. J. Doyle for stimulating discussions. Finally, we thank Dr. J. J. O'Malley and Mr. R. Hazelton for their support

and permission to publish this work. This work was done in its entirety at the Linden Technology Center, Exxon Chemical Co.

Appendix

Distribution of Composition. The papers by Stejskal et al.[30,31] describe how to calculate a number of important distribution functions for graft copolymers, such as the number of grafts per backbone chain. This is done for a broad range of molecular weight distributions of both the graft arms and the backbones. Here we apply their results on the distribution of composition, which is measured in terms of the fraction of backbone in a particular graft copolymer chain, x. This is of interest because these polymers fractionate primarily on the basis of composition, as shown above in Figure 6a–c. Thus the results of such fractionations should be directly related to calculations of the composition distribution.

This comparison is clearest if we compare the cumulative distribution of composition, $S(x)$, which is defined as the fraction of the graft copolymer that has composition x or less. We start with eq 36 in ref 31, which is valid when both the backbone and the graft arms are polydisperse in molecular weight:

$$W(x)\,dx = \frac{r^2 x_w(1-r)}{(1-r^2x_w)x}\,\frac{6Q^2(1-Q)}{[(1-Q)^2+4rQ]^{2.5}}\,dQ \quad (A.1)$$

where

$$Q = \frac{(1-x_w)}{(1-r)x_w}\,\frac{x}{(1-x)} \quad (A.2)$$

In eq 17 of ref 31, x_w is the weight-average value of x, m_n is the number-average number of grafts per molecule, and $r = (1 + m_n)^{-1}$. These last three parameters, x_w, m_n, and r, are all interrelated and are each a measure of the extent of grafting. All that is needed to determine the distributions is one of these three and the molecular weight distributions of the backbone and graft. In fact, for the composition distribution of the grafted polymer, all that is required is the ratio of the number-average molecular weights, α:

$$\alpha = M_{ng}/M_{nb} \quad (A.3)$$

where M_{ng} is the number-average molecular weight of the grafts, and M_{nb}, that of the backbones. Changing variables from Q to x gives

$$W(x)\,dx = \frac{6\alpha^2(1-x_w)}{(1-r^2x_w)}\,\frac{[(\alpha/r-1)x^2+x]}{[R(x)]^{2.5}} \quad (A.4)$$

where

$$R(x) = cx^2 + bx + 1 \quad (A.5)$$

$$c = (\alpha/r + 1)^2 - 4\alpha \quad (A.6)$$

$$b = 2(\alpha - 1/x_w) \quad (A.7)$$

To find the cumulative distribution, it is necessary to integrate $W(y)$ from 0 to x and normalize, so

$$S(x) = \frac{\int_0^x W(y)\,dy}{\int_0^1 W(y)\,dy} \quad (A.8)$$

$$= \frac{J(x)}{J(1)} \quad (A.9)$$

where

$$J(x) = [R(x)]^{-3/2}[(2cx^3 + 3bx^2)((\alpha/r-1)(b^2+4c) - 4cb) + (3bx+2)(4b(\alpha/r-1) - (b^2+4c))] - 2[4b(\alpha/r-1) - (b^2+4c)] \quad (A.10)$$

In Figure 5a–c the results of these calculations for grafts A–C are shown where it is assumed that all of each of the two components participated in the grafting; that is, x_w is equal to the weight fraction of the amine EP added to the reaction mixture. The agreement between the experimental data and these calculations supports the validity of this assumption.

References and Notes

(1) Plochocki, A. P. In *Polymer Blends*; Paul, D. R., Newman, S., Eds.; Academic Press: New York, 1978; Chapter 21.
(2) Kresge, E. N. In *Polymer Blends*; Paul, D. R., Newman, S., Eds.; Academic Press: New York, 1978; Chapter 20.
(3) Galli, P.; Danesi, S.; Simonazzi, T. *Polym. Eng. Sci.* **1984**, *24*, 544.
(4) Ranalli, R. *Dev. Rubber Technol.* **1982**, *3*, 21.
(5) Greco, R.; Martuscelli, E.; Ragosta, G.; Yin, J. *J. Mater. Sci.* **1988**, *23*, 4307.
(6) Lohse, D. J. *Polym. Eng. Sci.* **1986**, *26*, 1500.
(7) Inaba, N.; Sato, K.; Suzuki, S.; Hashimoto, T. *Macromolecules* **1986**, *19*, 1690.
(8) Inaba, N.; Yamada, T.; Suzuki, S.; Hashimoto, T. *Macromolecules* **1988**, *21*, 407.
(9) Maglio, G.; Palumbo, R. In *Polymer Blends*; Kryszewski, M., Galeski, A., Martuscelli, E., Eds.; Plenum: New York, 1982.
(10) Fayt, R.; Jerome, R.; Teyssie, P. *Makromol. Chem.* **1986**, *187*, 837.
(11) Noolandi, J.; Hong, K. M. *Macromolecules* **1984**, *17*, 1531.
(12) Brown, H. R.; Deline, V. R.; Green, P. F. *Nature* **1989**, *341*, 221.
(13) Anastasiadis, S. H., Koberstein, J. T. *Polym. Mater. Sci. Eng., Prepr.* **1988**, *58*, 634.
(14) Grace, H. P. *Chem. Eng. Commun.* **1982**, *14*, 225.
(15) Elmendorp, J. J.; van der Vegt, A. K. *Polym. Eng. Sci.* **1986**, *26*, 1332.
(16) Wu, S. *Polym. Eng. Sci.* **1987**, *27*, 335.
(17) Luckham, P. F. In *Polymer Surfaces and Interfaces*; Feast, W. J., Munro, H. S. Eds.; John Wiley & Sons: New York, 1987; Chapter 3, p 55.
(18) Wu, S. *Polymer* **1985**, *26*, 1855.
(19) Borggreve, R. J. M.; Gaymans, R. J.; Schuijer, J.; Ingen Housz, J. F. *Polymer* **1987**, *28*, 1489.
(20) Coran, A. Y.; Patel, R. *Rubber Chem. Technol.* **1983**, *56*, 1045.
(21) Simonazzi, T. *Pure Appl. Chem.* **1984**, *56*, 625.
(22) Lohse, D. J.; Datta, S.; Kresge, E. N. *Macromolecules* **1991**, *24*, 561.
(23) (a) Datta, S.; Kresge, E. N. (Exxon). U.S. Patent 4 987 200, 1990. (b) Datta, S. In *High Value Polymers*; Fawcett, A., Ed.; Royal Society of Chemistry: London, 1990; Chapter 2.
(24) Datta, S.; Morrar, F. T., to be published.
(25) Minoura, Y.; Ueda, M.; Mizunuma, S.; Oba, M. *J. Appl. Polym. Sci.* **1969**, *13*, 1625.
(26) *The Aldrich Library of Infra-Red Spectra*; Pouchert, C. J., Ed.; Aldrich Chemical Co.: Milwaukee, WI, 1989.
(27) Ver Strate, G.; Cozewith, C. A.; Ju, S. *Macromolecules* **1988**, *21*, 3360.
(28) Russ, J. C. In *Practical Stereology*; Plenum Press: New York, 1986.
(29) Schotte, Th. G. Characterization of Long Chain Branching in Polymers. In *Developments in Polymer Characterization–4*; Dawkins, J. V., Ed.; Elsevier: New York, 1983; Chapter 1.
(30) Stejskal, J.; Strakova, D.; Kratochvil, P.; Smith, S. D.; McGrath, J. E. *Macromolecules* **1989**, *22*, 861.
(31) Stejskal, J.; Kratochvil, P.; Jenkins, A. D. *Macromolecules* **1987**, *20*, 181.
(32) Stehling, F. C.; Huff, T.; Speed, C. S.; Wissler, G. E. *J. Appl. Polym. Sci.* **1981**, *26*, 2693.
(33) Bucknall, C. B. *Pure Appl. Chem.* **1986**, *58*, 999.